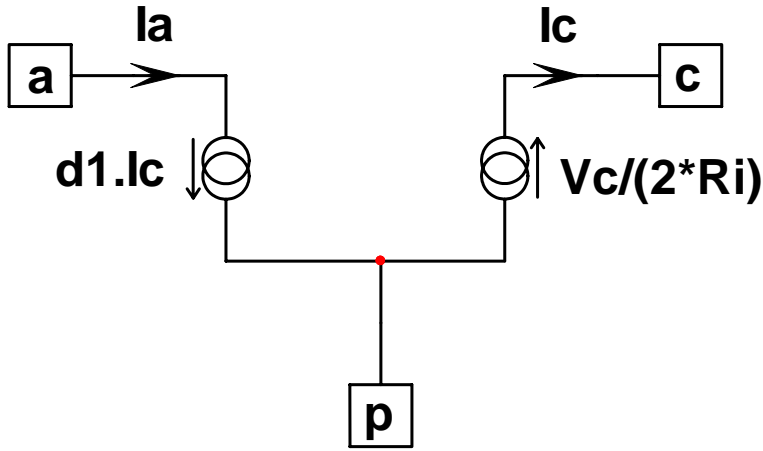


## A Small-Signal Analysis of the Current-Mode Borderline Conduction Mode PWM switch model

Christophe BASSO

On page 196 and fig. 2-104 of Ref. [1], appears a large-signal model of the PWM switch operated in the so-called quasi-square wave resonant mode. In order to analytically obtain the ac response of a current-mode flyback converter operated in the quasi-square wave resonant mode (also known as valley-switching operation), a new small-signal model has to be derived. First, let us try to simplify the large signal model given in Ref. [1]. In this model, the average current flowing in terminal “c” is written to stick to the PWM switch current-mode original notations: a main current source delivering a peak current equal to the control voltage  $V_c$  divided by the sense resistor  $R_i$  to which a source  $I_\mu$  subtracts some current. However, in a converter operated in Borderline Conduction Mode (BCM) where the dead time is negligible, the average current flowing through terminal “c” is simply the peak current value divided by 2. Capitalizing on this fact, the  $I_\mu$  source can disappear and an updated version of the large-signal model appears on figure 1:



**Figure 1:** the PWM switch model in Borderline Conduction Mode once simplified.

In this model, we have the following source definitions:

$$d_1 = \frac{V_c}{R_i} \frac{L}{V_{ac} T_{sw}} \quad (1)$$

$$T_{sw} = \frac{V_c L}{R_i} \left( \frac{1}{V_{ac}} + \frac{1}{V_{cp}} \right) \quad (2)$$

$$I_c = \frac{V_c}{2R_i} \quad (3)$$

$$I_a = d_1 I_c \quad (4)$$

If we use Eqs. (1) and (2) to develop Eq. (4), we have:

$$I_a = \frac{V_c}{R_i} \frac{L}{V_{ac} T_{sw}} I_c = \frac{I_c}{V_{ac} \left( \frac{1}{V_{ac}} + \frac{1}{V_{cp}} \right)} \quad (5)$$

The classical small-signal analysis requires the introduction of a perturbation on all the variables of the system. That is to say, we should transform equations Eqs. (3) and (5) by perturbing the following variables:

$$I_c = I_{c0} + \hat{i}_c \quad (6a)$$

$$I_a = I_{a0} + \hat{i}_a \quad (6b)$$

$$V_{cp} = V_{cp0} + \hat{v}_{cp} \quad (6c)$$

$$V_{ac} = V_{ac0} + \hat{v}_{ac} \quad (6d)$$

$$V_c = V_{c0} + \hat{v}_c \quad (6e)$$

The 0-indexed terms represent the dc point of the variable whereas the  $\hat{\phantom{x}}$  denotes the small ac variations around that dc point. Unfortunately, when you update the concerned variables into Eqs. (3) and (5), the exercise which consists of sorting out and gathering all the dc and ac terms becomes a rather tedious operation. One possible solution is to build an ac-only model, without any bias point capabilities. In this method, the ac terms are considered and the dc solutions are purposely left away. After all, we can always calculate the dc conditions either by using equations-based results or simply by running a bias point simulation with Fig. 1 large signal model. To obtain ac terms only, we can calculate the sensitivity of each current to the variables of concern listed in equations 6a to 6e. Let us apply this option to Eq. (3):

$$\hat{i}_c = \frac{\partial I_c}{\partial V_c} \hat{v}_c \quad (7)$$

$$\hat{i}_c = \hat{v}_c \left( \frac{1}{2R_i} \right) = \hat{v}_c k_c \quad (8)$$

Where  $k_c$  is simply:

$$k_c = \frac{1}{2R_i} \quad (9)$$

Let us apply a similar technique to equation (5) now:

$$\hat{i}_a = \frac{\partial I_a}{\partial V_{cp}} \hat{v}_{cp} + \frac{\partial I_a}{\partial I_c} \hat{i}_c + \frac{\partial I_a}{\partial V_{ac}} \hat{v}_{ac} \quad (10)$$

Once we derived Eq. (10), we obtain the following terms:

$$\hat{i}_a = \hat{v}_{cp} \frac{I_{c0} V_{ac0}}{(V_{ac0} + V_{cp0})^2} + \frac{V_{cp0}}{V_{cp0} + V_{ac0}} \hat{i}_c - \hat{v}_{ac} \frac{V_{cp0} I_{c0}}{(V_{ac0} + V_{cp0})^2} \quad (11)$$

Assuming:

$$k_{cp} = \frac{I_{c0} V_{ac0}}{(V_{ac0} + V_{cp0})^2} \quad (12a)$$

$$k_{ic} = \frac{V_{cp0}}{V_{cp0} + V_{ac0}} \quad (12b)$$

$$k_{ac} = \frac{V_{cp0} I_{c0}}{(V_{ac0} + V_{cp0})^2} \quad (12c)$$

we can re-write equation (11) the following way:

$$\hat{i}_a = \hat{v}_{cp} k_{cp} + \hat{i}_c k_{ic} - \hat{v}_{ac} k_{ac} \quad (13)$$

Re-arranging the original large-signal model with these new source definitions, the updated small-signal model appears in figure 2:

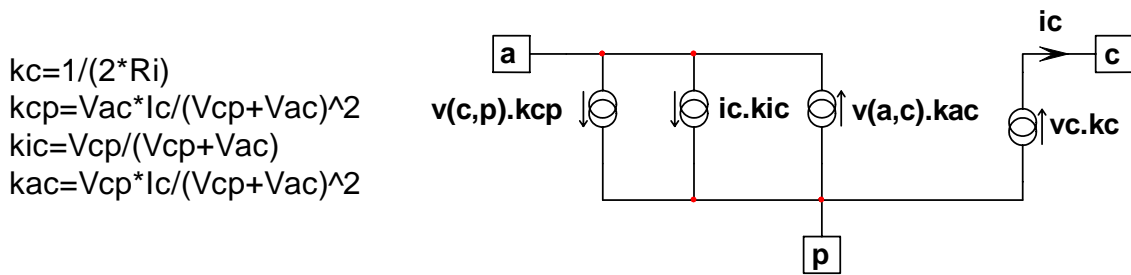


**Figure 2:** the updated small-signal model uses four current sources.

### A BCM flyback converter

Our main application is a flyback converter operated in Borderline Conduction Mode. The implementation of the BCM small-signal model in this configuration appears in figure 3:

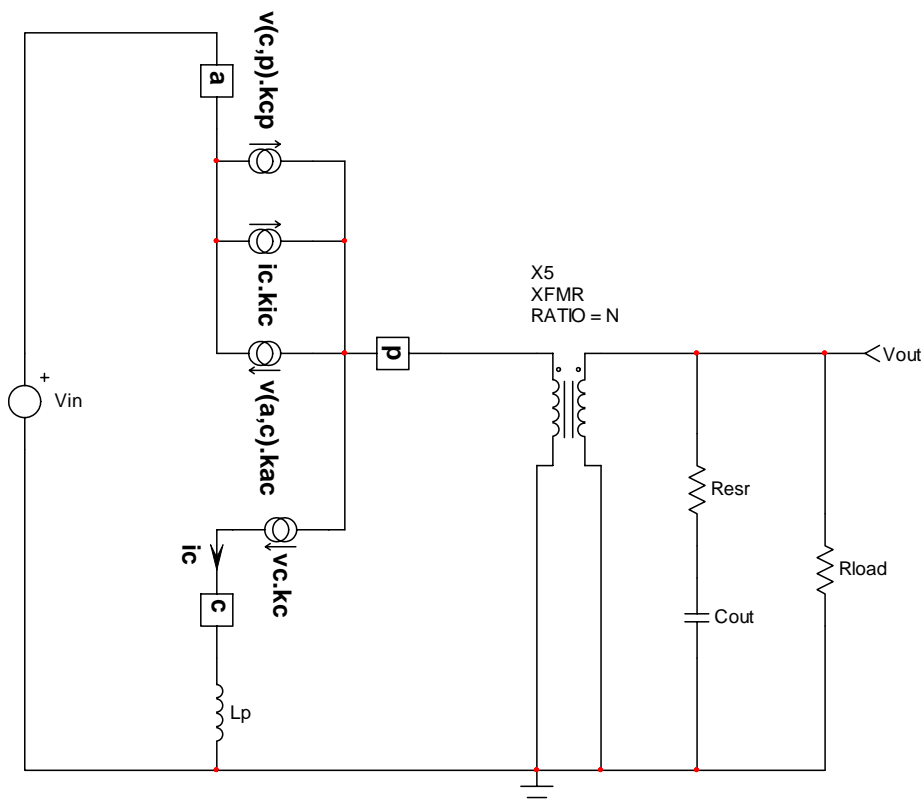


**Figure 3:** the small-signal model with a flyback converter.

In this application, observing the various terminal connections, we can update the coefficient definitions:

$$V_{ac0} = V_{in} \quad (14a)$$

$$V_{cp0} = \frac{V_{out}}{N} \quad (14b)$$

$$I_{c0} = \frac{V_{c0}}{2R_i} \quad (14c)$$

We can thus evaluate the coefficient parameters:

$$k_{cp} = \frac{V_{in} V_{c0}}{2R_i \left( V_{in} + \frac{V_{out}}{N} \right)^2} = \frac{V_{in} V_{c0} N^2}{2R_i (V_{out} + NV_{in})^2} \quad (15a)$$

$$k_{ic} = \frac{\frac{V_{out}}{N}}{\frac{V_{out}}{N} + V_{in}} = \frac{V_{out}}{V_{out} + NV_{in}} \quad (15b)$$

$$k_{ac} = \frac{\frac{V_{out}}{N} \frac{V_{c0}}{2R_i}}{\left( V_{in} + \frac{V_{out}}{N} \right)^2} = \frac{V_{out} V_{c0} N}{2R_i (V_{out} + NV_{in})^2} \quad (15c)$$

Using this configuration, let us find the dc small-signal gain  $G_0 \Big|_{\hat{v}_{in}=0} = \frac{\hat{v}_{out,s=0}}{\hat{v}_{c,s=0}}$ . First, since we are in

dc and  $V_{in}$  is considered constant during the study, terminal “a” goes to ground. Then, all capacitors are opened and the inductor is shorted: terminal “c” goes to ground as well. Since  $v(a,c)$  is null, the associated source disappears. Then, the load is reflected on the primary side using the transformer turns ratio squared. As a second observation, we can see that the current source involving  $k_{cp}$ , appears between the terminals “c” and “p”. Therefore, a resistance of value  $1/k_{cp}$  can be placed across the terminal “p” and ground. Finally, capitalizing on all these changes leads to the below equivalent schematic:

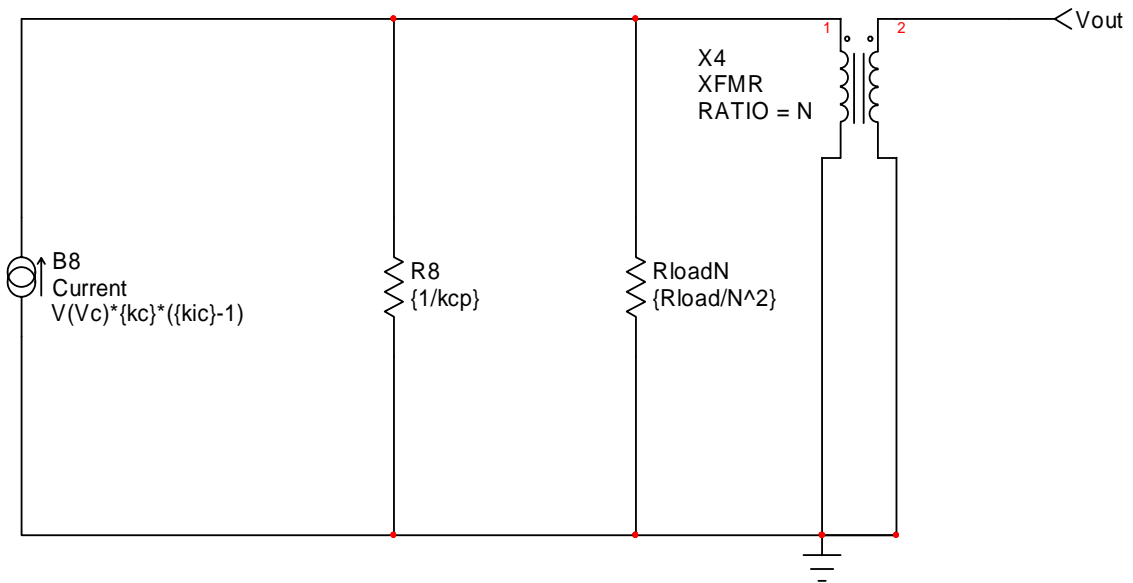


**Figure 4:** the dc small-signal gain is found by shorting the inductor and opening the capacitor. As  $V_{in}$  is constant, its small-signal value is 0.

The voltage appearing across  $R_8$  is equal to the current source value  $B_8$ , delivering current to the parallel combination of  $R_8$  and the reflected load. Let's call  $R_{eq}$  this compound resistor:

$$R_{eq} = \frac{R_{load}}{N^2} \parallel \frac{1}{k_{cp}} = \frac{R_{load}}{R_{load}k_{cp} + N^2} \quad (16)$$

The small-signal output voltage equation is therefore:

$$\hat{v}_{out,s=0} = \hat{v}_{c,s=0}k_c(1-k_{ic})R_{eq}N \quad (17)$$

In the above equation, the minus sign passed to the transformer turns ratio – our flyback delivers a positive voltage, whereas a buck-boost gives a negative output – has been included in the expression. From Eq. (17), we can derive the dc gain of the BCM flyback:

$$G_0 = k_c(1-k_{ic})R_{eq}N \quad (18)$$

### Application example

A simple open-loop flyback has been wired using the PWM switch model described in Ref. [1]. This a converter delivering 19.2 V to a 10  $\Omega$  load from a 100-Vdc input source. The control voltage is set to 1.7 V and imposes a 1.7 A peak current.

#### parameters

**Vin=100**  
**Rload=10**  
**N=-0.25**  
**ESR=1**  
**Cout=100u**  
**Lp=1m**  
**Vc=1.7**  
**Ri=1**  
**Fsw=25.6k**

**Ic=Vc/(2\*Ri)**  
**Vac=100**  
**Vcp=76.9**

**kc=1/(2\*Ri)**  
**kcp=Vac\*Ic/(Vcp+Vac)^2**  
**kic=Vcp/(Vcp+Vac)**  
**kac=Vcp\*Ic/(Vcp+Vac)^2**

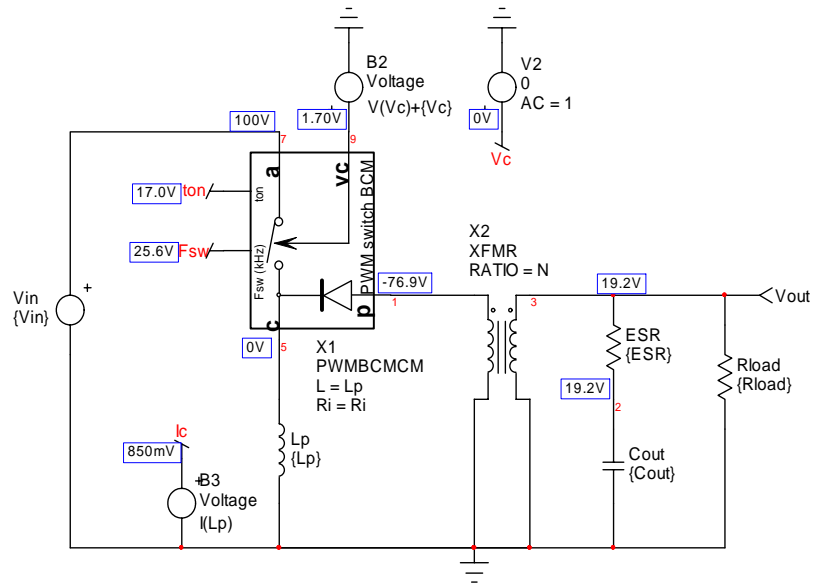


**Figure 5:** a large-signal simulation of a BCM flyback converter running open-loop.

From the above dc points, we can calculate our source coefficients:

$$k_{cp} = \frac{V_{in} V_{c0} N^2}{2R_i (V_{out} + NV_{in})^2} = \frac{100 \times 1.7 \times 0.25^2}{2 \times 1 \times (19.2 + 0.25 \times 100)^2} = 2.72m \quad (19a)$$

$$k_{ic} = \frac{V_{out}}{V_{out} + NV_{in}} = \frac{19.2}{19.2 + 0.25 \times 100} = 434m \quad (19b)$$

$$k_{ac} = \frac{V_{out} V_{c0} N}{2R_i (V_{out} + NV_{in})^2} = \frac{19.2 \times 1.7 \times 0.25}{2 \times 1 \times (19.2 + 0.25 \times 100)^2} = 2.09m \quad (19c)$$

$$k_c = \frac{1}{2R_i} = \frac{1}{2 \times 1} = 0.5 \quad (19d)$$

The equivalent resistor is found to be:

$$R_{eq} = \frac{R_{load}}{R_{load} k_{cp} + N^2} = \frac{10}{10 \times 2.72m + 0.25^2} = 111.49 \Omega \quad (20)$$

The dc gain is derived using Eq. (18):

$$G_0 = 20 \log_{10} (k_c (1 - k_{ic}) R_{eq} N) = 20 \log_{10} (0.5 \times (1 - 0.434) \times 111.49 \times 0.25) = 17.93 \text{ dB} \quad (21)$$

If we run Fig. 5 simulation template, we obtain the below gain curve:

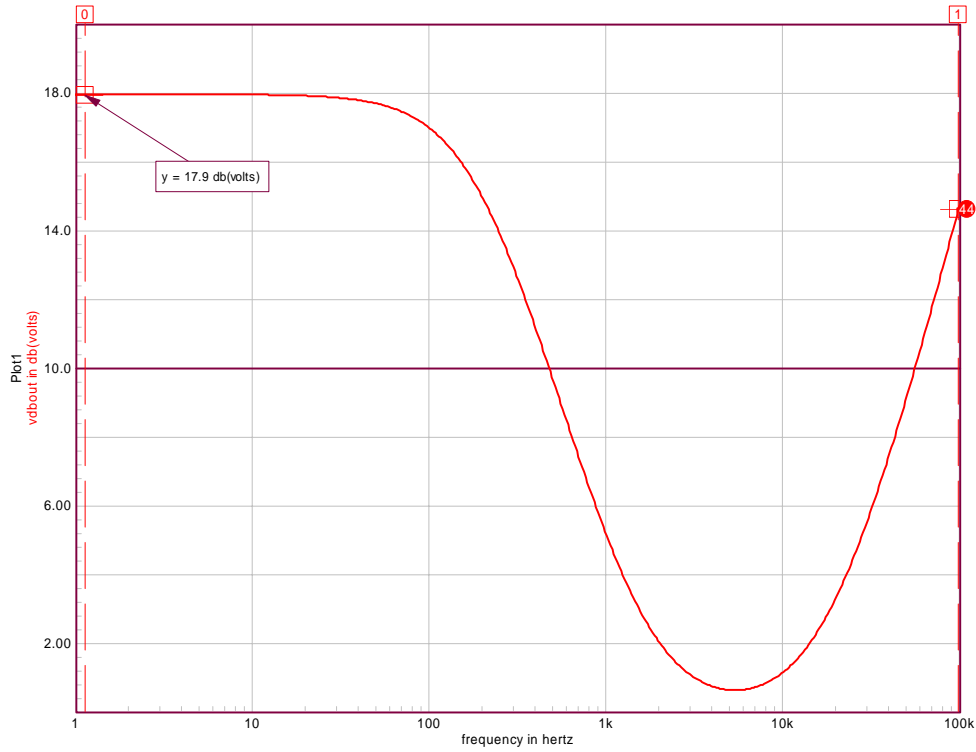


**Figure 6:** the dc gain given by the linearized large-signal model sticks to the result given by Eq. (21).

### Ac analysis

The control to output ac analysis implies that inductors and capacitors are back in place as in Fig. 3. The new schematic appears in Fig. 7.

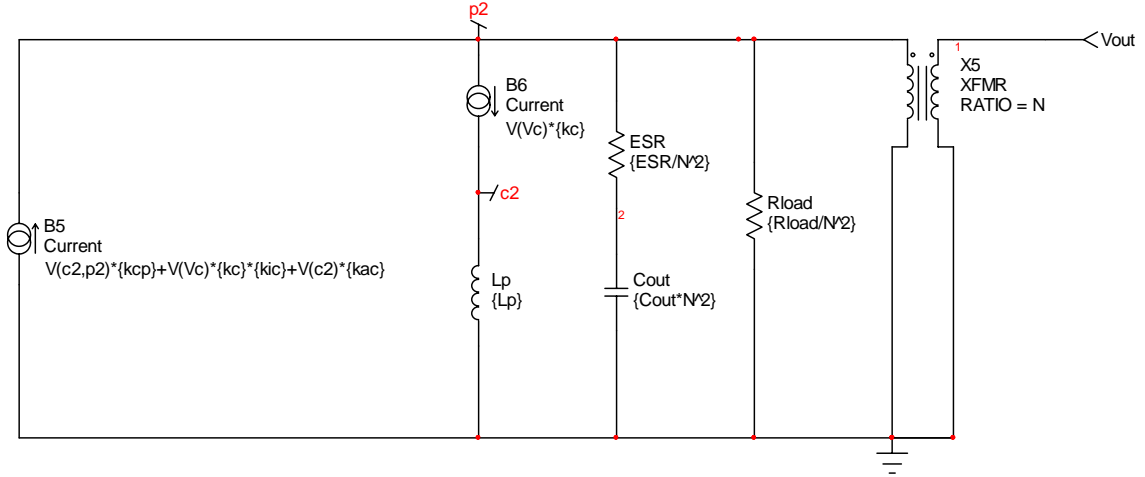


**Figure 7:** the elements are back in place for the ac analysis.

The schematic looks a bit complicated at the first glance, but a careful writing of the equations will lead us to the correct result rather quickly. In Fig. 7, we can see a current source  $B_5$  delivering current to complex impedance made of the reflected capacitor, its ESR and the load resistor. However,  $B_5$  current is diverted into the inductor by  $B_6$ . The equation of the output voltage is thus:

$$V(c_2, p_2)k_{cp} = -V(p_2, c_2)k_{cp} = -\left(-\frac{\hat{v}_{out}(s)}{N} - sL_p \hat{i}_c\right)k_{cp} = \left(\frac{\hat{v}_{out}(s)}{N} + sL_p \hat{v}_c(s)\right)k_{cp} \quad (22)$$

$$-\left[\frac{\hat{v}_{out}(s)}{N}k_{cp} + \hat{v}_c(s)k_c k_{cp} sL_p + \hat{v}_c(s)k_c k_{ic} + \hat{v}_c(s)k_c k_{ac} sL_p - \hat{v}_c(s)k_c\right]Z(s)N = \hat{v}_{out}(s) \quad (23)$$

$$-\hat{v}_c(s)k_c \left[sL_p(k_{cp} + k_{ac}) + k_{ic} - 1\right]Z(s)N = \hat{v}_{out}(s) + \frac{\hat{v}_{out}(s)}{N}k_{cp}Z(s)N \quad (24)$$

$$-\hat{v}_c(s)k_c \left[sL_p(k_{cp} + k_{ac}) + k_{ic} - 1\right]Z(s)N = \hat{v}_{out}(s) \left[1 + k_{cp}Z(s)\right] \quad (25)$$

$$\hat{v}_c(s)k_c \left[1 - k_{ic} - sL_p(k_{cp} + k_{ac})\right]N \frac{Z(s)}{1 + k_{cp}Z(s)} = \hat{v}_{out}(s) \quad (26)$$

Factoring  $1 - k_{ic}$ :

$$\hat{v}_c(s)Nk_c(1 - k_{ic}) \left[1 - sL_p \frac{k_{cp} + k_{ac}}{1 - k_{ic}}\right] \frac{Z(s)}{1 + k_{cp}Z(s)} = \hat{v}_{out}(s) \quad (27)$$

The transfer function now comes easily:

$$\frac{\hat{v}_{out}(s)}{\hat{v}_c(s)} = Nk_c(1 - k_{ic}) \left[1 - sL_p \frac{k_{cp} + k_{ac}}{1 - k_{ic}}\right] \frac{Z(s)}{1 + k_{cp}Z(s)} \quad (28)$$

The term  $k_{cp}Z(s)$  combines reflected elements on the primary side. Let's see how to derive it:

$$k_{cp}Z(s) = k_{cp} \frac{\frac{R_{load}}{N^2} \left( \frac{R_{ESR}}{N^2} + \frac{1}{sC_{out}N^2} \right)}{\frac{R_{load}}{N^2} + \left( \frac{R_{ESR}}{N^2} + \frac{1}{sC_{out}N^2} \right)} \quad (29)$$

Developing and re-arranging all terms gives:

$$\frac{Z(s)}{1+k_{cp}Z(s)} = \frac{1}{k_{cp} + \frac{N^2}{R_{load}}} \frac{1+sR_{ESR}C_{out}}{1+sC_{out} \left( \frac{N^2 + \frac{N^2R_{ESR}}{R_{load}} + k_{cp}R_{ESR}}{k_{cp} + \frac{N^2}{R_{load}}} \right)} \quad (30)$$

Introducing this expression into the small-signal gain we have derived (Eq. (28)) gives:

$$\frac{\hat{v}_{out}(s)}{\hat{v}_c(s)} = \frac{Nk_c(1-k_{ic})}{k_{cp} + \frac{N^2}{R_{load}}} \frac{(1+sR_{ESR}C_{out}) \left( 1 - sL_p \frac{k_{cp} + k_{ac}}{1-k_{ic}} \right)}{1+sC_{out} \left( \frac{N^2 + \frac{N^2R_{ESR}}{R_{load}} + k_{cp}R_{ESR}}{k_{cp} + \frac{N^2}{R_{load}}} \right)} = G_0 \frac{\left( 1 + \frac{s}{s_{z1}} \right) \left( 1 - \frac{s}{s_{z2}} \right)}{\left( 1 + \frac{s}{s_{p1}} \right)} \quad (31)$$

From this expression, we can identify:

$$G_0 = \frac{Nk_c(1-k_{ic})}{k_{cp} + \frac{N^2}{R_{load}}} \quad (32)$$

A left-half plane zero:

$$s_{z1} = \frac{1}{R_{ESR}C_{out}} \quad (33)$$

A right-half place zero:

$$s_{z2} = \frac{1-k_{ic}}{(k_{cp} + k_{ac})L_p} = \frac{1}{L_p \frac{V_c}{2R_i V_{in}}} \quad (34)$$

A pole:

$$s_{p1} = \frac{1}{C_{out} \left( \frac{N^2 + \frac{N^2R_{ESR}}{R_{load}} + k_{cp}R_{ESR}}{k_{cp} + \frac{N^2}{R_{load}}} \right)} \quad (35)$$



Entering Eq. (35) into Mathcad gives us the complete ac picture:

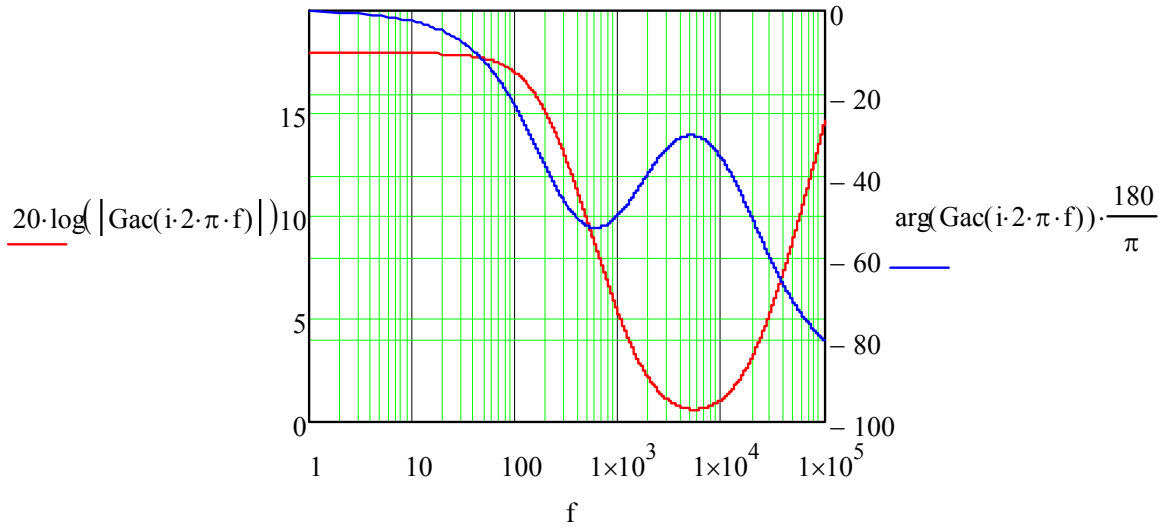


**Figure 8:** the small-signal plot of Eq. (31) using Mathcad.

### Numerical application

If we now use the numerical values calculated for the various coefficients, based on Fig. 5 schematic, we can locate the following poles and zeros:

$$G_0 = 17.9 \text{ dB} \quad (36a)$$

$$f_{z1} = 1.59 \text{ kHz} \quad (36b)$$

$$f_{z2} = 18.7 \text{ kHz} \quad (36c)$$

$$f_{p1} = 199.7 \text{ Hz} \quad (36d)$$

If we neglect the ESR contribution to Eq. 36d, the new pole is positioned at  $f_{p1} = 228 \text{ Hz}$ .

Reference [2] describes the derivation of BCM structures using the loss-free network concept. The given expressions for the gain, pole and zeros are the following:

$$G_0 = 20 \log_{10} \frac{R_{load} N}{2N^2 \left( 2 \frac{V_{out}}{NV_{in}} + 1 \right)} = 20 \log_{10} \frac{10}{2 \times 0.25 \times \left( \frac{19.2 \times 2}{0.25 \times 100} + 1 \right)} = 17.93 \text{ dB} \quad (37)$$

$$f_{p1} = \frac{1}{2\pi R_{load} C_{out}} \frac{2M+1}{M+1} = \frac{1}{6.28 \times 10 \times 100 \mu} \times \frac{2 \frac{19.2}{0.25 \times 100} + 1}{\frac{19.2}{0.25 \times 100} + 1} = 228 \text{ Hz} \quad (38)$$

$$f_{z2} = \frac{R_{load}}{N^2 2\pi L_p} \frac{1}{M(1+M)} = \frac{10}{0.25^2 \times 6.28 \times 1m} \frac{1}{\frac{19.2}{0.25 \times 100} \left( 1 + \frac{19.2}{0.25 \times 100} \right)} = 18.7 \text{ kHz} \quad (39)$$

Reference [2] did not consider the ESR of the capacitor in the derivation of the models. Eq. (36b) does not change.

The full ac simulation, including phase and gain appears in Fig. 9 where we have purposely added in the background, the Mathcad plot:

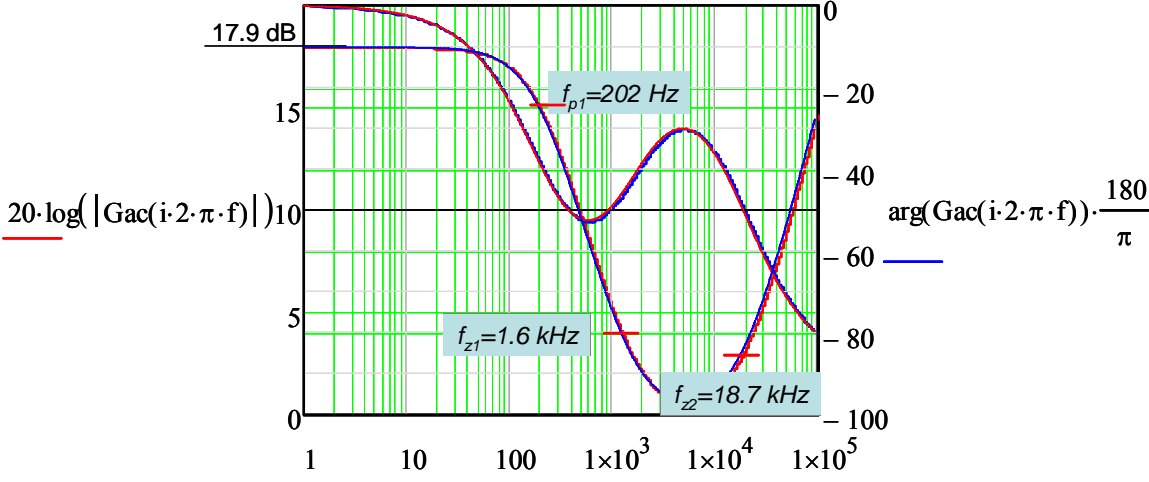


**Figure 9:** the comparison between the Bode plot given by the SPICE simulation of the non-linear BCM model as applied in Fig. 5 and the Mathcad transfer function.

As one can see, both plots perfectly superimpose on each other showing the validity of the approach described here.

**References**

1. Christophe Basso, “Switch-Mode Power Supplies: SPICE Simulations and Practical Designs”, McGraw-Hill, 2008.
2. J. Chen, B. Erickson, D. Maksimović, “Average Switch Modeling of Boundary Conduction Mode Dc-to-Dc Converters, Proc. IEEE Industrial Electronics Society Annual Conference (IECON 01), Nov. 2001, vol. 2, pp. 842-849.